DEPARTMENT OF ELECTRONIC & ELECTRICAL ENGINEERING

University of Strathclyde Engineering

EE467 Semester 2 Assignment

Liam Tang | 202135591

EE467: Power System Design, Operation And Protection

Date: March 14, 2025

I hereby declare that this work has not been submitted for any other degree/course at this University or any other institution and that, except where reference is made to the work of other authors, the material presented is original and entirely the result of my own work at the University of Strathclyde.

1. Transformer differential protection

1.i. Protection design and settings

1.i.1. Yd9 Phasor and Connection Diagram

The phasor diagram for the Yd9 connection group commences with the appreciation of the star and delta configurations. In this instance, the High Voltage (HV) primary side of the transformer is star connected and the Low Voltage (LV) secondary side is delta. This is visualised in Figure 1 where the convention is adopted where capital letters denote primary side phases, lower case letters are indicative of the secondary side phases, and the phases are named as A,B,C. It is worth noting that x,y,z are representative of the internal transformer side for HV and LV.

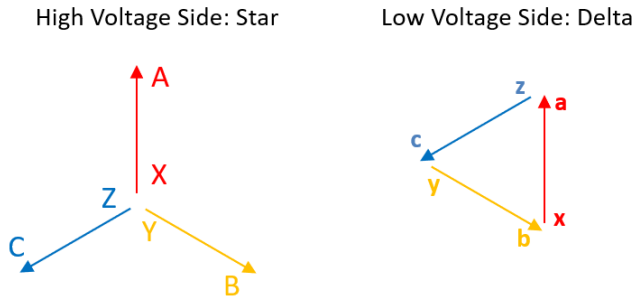

Figure 1: Transformer Phasor Diagram

The method continues by finding the star equivalent for the LV delta side - this is denoted by the dotted lines. From the Yd9 connection group, it is understood that a phase shift of 9 hours is desired. This hourly shift notion is taken from the clock face where each hour is 30 degrees. Phase A on the HV side can be taken as reference here, with an angle of 0 degrees, or at 12 o'clock. The desired transformation states that a shift from HV to LV of 9 hours or 270 degrees is desired in the clockwise direction. Hence, the star equivalent LV side is illustrated in Figure 2.

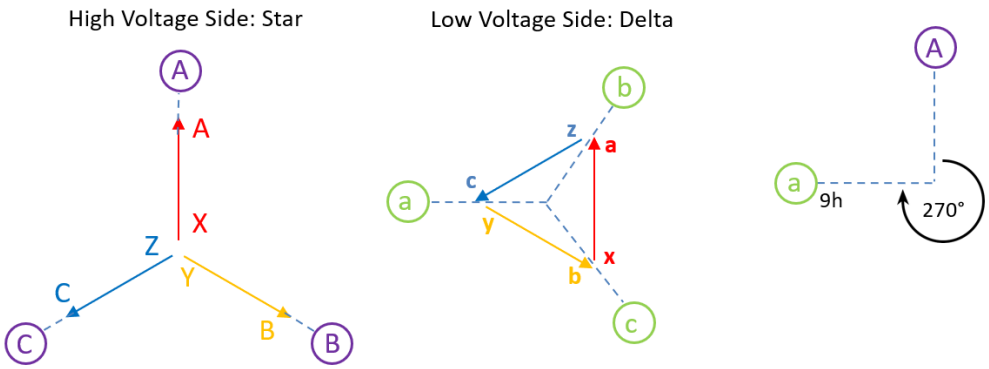

Figure 2: Yd9 Phasor Diagram

The phasor diagram serves as a critical blueprint for the design of the connection diagram that describes the wiring of the power transformers, current transformers, and secondary side relay phases.

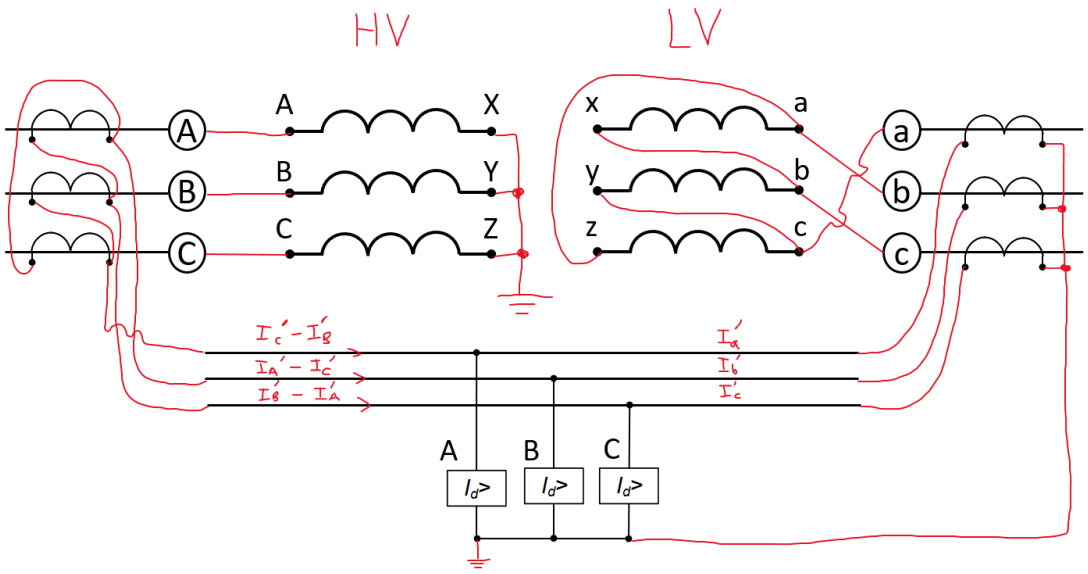

Figure 3: Transformer and Relay Connection Diagram

The connections for the internal side of the transformer is simple as this purely depends on the star or delta nature of the transformer. Connecting the external side to the line phases A,B,C requires more attention. On the HV side, connections from the transformer to the line phases begins with the inspection of the HV side phasor diagram in Figure 2. The purple phases are in alignment with those on the HV side, and so the connections can be made accordingly. A similar process is carried out on the LV side where the phasor diagram states that the following connections should be made for the Yd9 transformation to be complete. Namely, these are: a $\rightarrow$ b, c $\rightarrow$ a, b $\rightarrow$ c.

Lastly, connections of the current transformers (CTs) on the line are made. These follow the same connections that are made between the line and transformer phases on the opposite power transformer side. For example, the HV CTs are connected to the referred relay line in the same manner that the LV power transformer is connected to the phases of the transmission line. The opposite is true for the LV CTs where the phases are simply matched up. The final transformer wiring diagram is displayed in Figure 3.

1.i.2. Selection of Current Transformer Ratios

The expression for the HV and LV side transformer nominal currents can be calculated as

$$I_{nH} = \frac{S_n}{\sqrt{3}V_H} = \frac{60 \times 10^6}{\sqrt{3} \times 275 \times 10^3} = \underline{\mathbf{126A}} \tag{1}$$

and

$$I_{nL} = \frac{S_n}{\sqrt{3}V_H} = \frac{60 \times 10^6}{\sqrt{3} \times 33 \times 10^3} = \underline{\mathbf{1050A}} \tag{2}$$

Thus the selection of CT ratio for the HV side is computed as

$$N_{CTH} \geq \sqrt{3}I_{nH} = \sqrt{3} \times 126 = \underline{\mathbf{218.24}} \tag{3}$$

and so the appropriate available CT ratio is $\underline{\mathbf{N_{CTH} = 250 : 1}}$ Note, the root 3 can be used here since it is assumed that the 3-phase system is balanced. The same approach is taken for the LV side.

$$N_{CTL} \geq I_{nH} = \underline{\mathbf{1050}} \tag{4}$$

From the available list, the most fitting ratio is $\underline{\mathbf{N_{CTL} = 1250 : 1}}$

1.i.3. Setting Current Selection

A similar expression for the high side transformer nominal current is given as

$$I_{nH} = \frac{S_n}{\sqrt{3} \times 0.85V_H} = \frac{60 \times 10^6}{\sqrt{3} \times 0.85 \times 275 \times 10^3} = \underline{\mathbf{148.2A}} \tag{5}$$

Notice the slight modification made here is the inclusion of the $\pm 15\%$ tap changer. The selection of 0.85 was used as the maximum steady state spill current is desired and a smaller voltage maximises I_{nH}. The spill current is calculated as follows

$$I_{spill=} \left| \frac{\sqrt{3}I_{nH}}{N_{CTH}} - \frac{I_{nL}}{N_{CTL}} \right| = \left| \frac{\sqrt{3} \times 148.2}{250/1} - \frac{1050}{1250/1} \right| = 0.186759\ldots \tag{6}$$

The guidelines in the assignment brief state that the first setting current should be at least four times the maximum steady state spill current at full transformer load. This is modelled and solved in (7).

$$I_{S1} \geq 4I_{spill} = 4 \times 0.186759 \cdots = 0.747A \tag{7}$$

Therefore, the first setting current is chosen as $I_{S1} = \underline{\mathbf{0.75A}}$ from the available setting values. It is worth noting that the setting current was rounded up since if rounded down, it would infer that the spill current

and nominal transformer current is lower, suggesting that the maximum steady state spill current is not used in this condition.

The guideline for the second setting current I_{S2} indicates it should be 1.1 times greater than the transformer rated current. The high side current is calculated as

$$I_{nH}\prime = \frac{I_{nH}\sqrt{3}}{N_{CT1}} = \frac{126}{250} = 0.873A \tag{8}$$

The inclusion of the root 3 is required for star referrals onto the secondary side. Likewise, the low side is calculated in the following way

$$I_{nL}\prime = \frac{I_{nH}}{N_{CT1}} = \frac{1050}{1250} = 0.84A \tag{9}$$

Taking the maximum of these values, the second setting current is finally calculated.

$$I_{S2} = 1.1I_{nH}\prime = 1.1 \times 0.873 = \underline{\mathbf{0.9603A}} \tag{10}$$

1.ii. Differential Protection Operation

The differential operation study considers fault cases 1 and 2. The transformer primary line currents during the faults are captured in the assignment brief document and are defined in a direction towards the transformer. It was decided that the fault cases adopted the naming convention where the number denotes the case, and the letter is representative of the phase of the case, as displayed in the first column of Table 1.

Analysis of the transformer connection diagram in Figure 3 indicates that Kirchoff's Current Law is exploited on the HV side, yielding the population of column I_1 when referred using the appropriate CT ratio N_{CTH}. The same is applied to the LV side, where the connection diagram indicates that referral to the secondary side only requires division by N_{CTL}, thus providing an expression for I_2 in each case. The differential and bias currents are calculated using characteristic equations (11) and (12).

$$I_{diff} = |I_1 + I_2| \tag{11}$$

$$I_{bias} = \frac{|I_1| + |I_2|}{2} \tag{12}$$

These can then be used to determine whether tripping occurs for each instance by using the dual-slope

tripping equation (13)

$$Trip = (I_{diff} > I_{S1} + k_1 I_{bias}) \wedge (I_{diff} > I_{S1} + (k_1 - k_2) I_{S2} + k_2 I_{bias}) \tag{13}$$

which states that the first term will be used if $I_{bias} < I_{S2}$ and the second term will be used in all other circumstances. To showcase the steps involved with determining whether a trip occurs, the step-by-step calculation for the 1(A) fault case is computed. Firstly, I_1 is calculated as:

$$I_1 = I_{C\prime} - I_{B\prime} = \frac{(297.33\angle 141.96) - (248.97\angle 167.84)}{250} = 0.0369 + j0.523A \tag{14}$$

Next, I_2 is calculated

$$I_2 = \frac{I_a}{N_{CT2}} = \frac{550.77\angle -94.26}{1250} = -0.0327 - j0.439A \tag{15}$$

Which enables the subsequent computation of I_{diff} and I_{bias}

$$I_{diff} = |I_1 + I_2| = |(0.0369 + j0.523) + (-0.0327 - j0.439)| = 0.0841A \tag{16}$$

$$I_{bias} = \frac{|(0.0369 + j0.523)| + |(-0.0327 - j0.439)|}{2} = 0.4825A \tag{17}$$

Since I_{bias} is less than I_{S2}, then the first expression in the tripping condition is used

$$I_{S1} + k_1 I_{bias} = 0.75 + 0.1 \times 0.4825 = 0.798A \tag{18}$$

which is less than I_{diff}, hence Fault Case 1(A) **does not trip**. Table 1 conveniently summarises the results from this study where the calculations shown above were automated using a script that iterated through every case.

Fault Case	Relay Side Phase	$\mathbf{I_1}$	$\mathbf{I_2}$	$\mathbf{I_{diff}(A)}$	$\mathbf{I_{bias}(A)}$	Trip Flag
1 (A)	A	$I_C\prime - I_B\prime$	$I_a\prime$	0.08	0.48	0
1 (B)	B	$I_A\prime - I_C\prime$	$I_b\prime$	0.18	3.21	0
1 (C)	C	$I_B\prime - I_A\prime$	$I_c\prime$	0.16	3.03	0
2 (D)	A	$I_C\prime - I_B\prime$	$I_a\prime$	2.70	1.40	1
2 (E)	B	$I_A\prime - I_C\prime$	$I_b\prime$	0.09	0.56	0
2 (F)	C	$I_B\prime - I_A\prime$	$I_c\prime$	2.71	1.37	1

Table 1: Dual-slope differential protection quantitative summary

Figure 4 displays this graphically, where the shaded red area is the tripping region, the blue line is the dual-slope boundary, and the shapes are the different cases. Interpreting these findings leads to the conclusion that Fault Case 1 is an external fault, as the differential protection method only safeguards the specific unit it is applied to and none of the cases caused the relay to trip, indicating that the fault occurs outside the protection zone. On the contrary, Fault Case 2 represents an internal fault since the relays trip for relay side phases A and C.

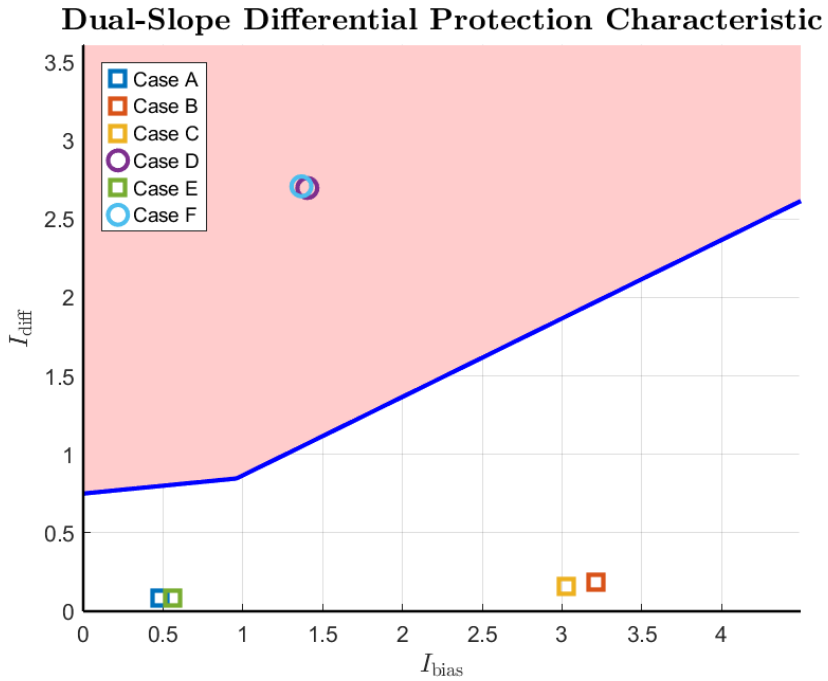

Figure 4: Graphical display of the Dual-slope Differential Protection Characteristic

2. System Stability and Control

2.i. Power system stability classification and analysis

Stability in the context of power systems means the performance of a power system when transitioning between steady-state conditions due to an interruption [1]. Table 2 discusses the different stability types in

detail where information was sourced from [1] and [2].

Stability Type	**Definition**	**Analysis Purpose**	**Time Period of Interest**	**Analysis Method**
Steady-State	The ability of the system to maintain equilibrium under gradual changes in load or operating conditions.	Ensure phase angle and voltage levels are within acceptable limits, check for overloading during heavy loading instances	Hours after disturbance has settled	Power-flow computer analysis (e.g., PowerFactory), Gauss-Siedel
Transient	Transient cases are concerned with major disturbances like loss of generators, lines, switching, faults, and immediate load changes	Discover if system retains synchronism after such disturbances	The first few seconds after the event	Time-domain simulations (Numerical Integration methods i.e. Euler, Runge-Kutta)
Dynamic (Small-Signal)	The system's ability to recover and maintain synchronism after a small disturbance	Study how controls such as turbine-governors, excitation systems, and dispatch center controls stabilize or destabilize the power system.	Several minutes after disturbance occurs	Power-flow computer analysis (e.g., PowerFactory), utilisation of state-space models
Voltage	The ability to maintain steady-state voltages across all of the system post disturbances	Understand the short term and long term phenomena. Short term looks at fast-acting components like HVDC links and asynchronous machines. Long term looks at slower components like tapchangers on transformers	Seconds to minutes after disturbance	Analysing reactive power balance and load characteristics, PV and QV curves, load flow studies
Frequency	The power system's ability to preserve a steady frequency	Study how the system restores balance between demand and generation	Seconds to a few minutes after disturbance	Governor response analysis to understand the mechanisms that control the synchronous machines and Eigenvalue analysis to better understand unstable frequency modes. Furthermore, the ROCOF method is used to measure the frequency change with time [3]

Table 2: Power System Stability Classification

2.ii. Steady-state Power Limit

The total reactance in the system can be found by summing the reactance from the generator, first transformer, line, second transformer, and the synchronous motor.

$$X_{TOTAL} = X_G + X_{TR1} + X_{line} + X_{TR2} + X_m = 1 + 0.1 + 0.1 + 0.125 + 1 = 2.325pu \tag{19}$$

The steady-state power limit in per unit is given and solved using

$$P_{max_{pu}} = \frac{E_G E_M}{X_{TOTAL}} = \frac{1.1 \times 1}{2.325} = 0.473pu \tag{20}$$

Finally, this can be converted into SI units by multiplying by S_{BASE},

$$P_{max_{SI}} = P_{max_{pu}} \times S_{BASE} = 0.473 \times 100M = \underline{\mathbf{47.3MVA}} \tag{21}$$

2.iii. Critical clearing time

The critical clearing time problem can be better represented on a $p - \delta$ plot where the power is measured in the per unit system, and the power angle delta is measured in radians. This is displayed in Figure 5.

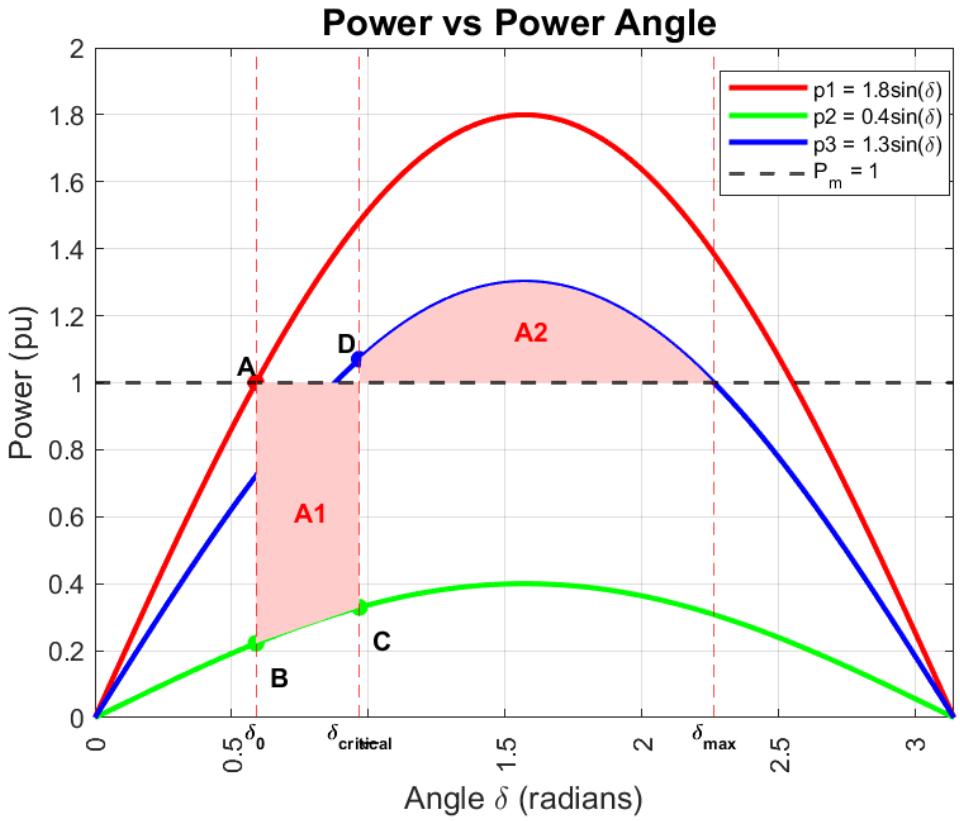

Figure 5: Power vs Power Angle

The 3 curves represent the electrical power under different scenarios with p1 being before the fault, p2 during the fault, and p3 after the fault. The parameters given in the question are conveniently displayed in Table 3.

Parameter Name	Value
Mechanical Power, P_m	1 pu
Pre-fault maximum Electrical Power, P_1	1.8 pu
During-fault maximum Electrical Power, P_2	0.4 pu
Post-fault maximum Electrical Power, P_3	1.3 pu
Inertia Constant, H	4.5s
Frequency, f	50Hz

Table 3: Parameters given in question

The critical clearing angle is the maximum variation in the load angle curve that occurs before a fault is cleared, without inducing a loss of synchronism. Similarly, the critical clearing time represents the longest fault duration for stability to still be possible. Times greater than this cause area 1 to be greater than area 2 which leads to an unstable system [4].

The angle δ_0 is calculated by equating the mechanical power of the generator with the pre-fault power curve, p1. This solves to give point **A**:

$$\delta_0 = \sin^{-1}(\frac{P_m}{P_{max1}}) = \sin^{-1}(\frac{1}{1.8}) = 0.589\,\text{rad} \tag{22}$$

The same can be achieved for the angle δ_{max}

$$\delta_{max} = \pi - \sin^{-1}(\frac{P_m}{P_{max3}}) = \pi - \sin^{-1}(\frac{1}{1.3}) = 2.264\,\text{rad} \tag{23}$$

The critical clearing angle is solved by using the equal area criterion which states that stability occurs when the power deficit during the fault is equal to the power surplus after the fault [5]. Thus, areas 1 and 2 must be equal and the critical angle can be solved as

$$\int_{\delta_0}^{\delta_{cr}} (P_m - P_{max2}\sin\delta)\,d\delta = \int_{\delta_{cr}}^{\delta_{max}} (P_{max3}\sin\delta - P_m)\,d\delta \tag{24}$$

Substitution of known variables and rearranging for the critical angle gives:

$$\delta_{cr} = \underline{\mathbf{0.96697}\,\text{rad}} \tag{25}$$

The critical clearing time can be calculated by solving a reformulated version of the swing equation which captures the acceleration modelled as the difference between the mechanical power and electrical power.

$$\frac{2H}{W_s}\frac{d^2\delta(t)}{dt^2} = 1 - 0.4\sin\delta(t) \tag{26}$$

The electrical power evolves with the power angle, which evolves with time, explaining the notation for the above equation. The initial case for this states that at t=0, $\delta(0) = 0.589$ radians and it is also known that the angle at the critical time is $\delta(t_{cr})$ = 0.96697; thus calculating the critical clearing time requires solving a non-linear ordinary differential equation. This was computed in matlab using a control theory estimation technique since this problem can be reformulated as a state-space equation. Running the code gives:

$$t_{cr} = \underline{\mathbf{0.1670s}} \tag{27}$$

A sanity check can be executed by using the Runge-Kutta numerical integration method to solve the ODE in (26). The code for this is displayed in Listing 1 and this yielded a final critical time of $\underline{t_{cr}}$ **= 0.1691s**. Both methods are in alignment, with slight differences in final results due to the accuracy of the approximation techniques used.

```
clc;
clear;

% define parameters
H = 4.5;
w_syn = 2 * pi * 50;
delta_0 = 0.589;
delta_tc = 0.96697;

% Define the system of ODEs
f1 = @(delta_2) delta_2;
f2 = @(delta_1) (w_syn / (2 * H)) * (1 - 0.4 * sin(delta_1));

% time span and initial conditions
t_max = 0.5;
h = 0.0000001; %choosing a low step size for granularity
t = 0:h:t_max;
y0 = [delta_0; 0];

% initialise arrays to store the results
delta1_vals = zeros(1, length(t)); % For delta(t)
delta2_vals = zeros(1, length(t)); % For d(delta)/dt
delta1_vals(1) = y0(1);
delta2_vals(1) = y0(2);

% Runge-Kutta 4th-order method
for i = 1:length(t)-1
    % Current values
    delta1 = delta1_vals(i);
    delta2 = delta2_vals(i);

    % Compute the RK4 coefficients
    k1_1 = f1(delta2);
    k1_2 = f2(delta1);

    k2_1 = f1(delta2 + 0.5*h*k1_2);
    k2_2 = f2(delta1 + 0.5*h*k1_1);

    k3_1 = f1(delta2 + 0.5*h*k2_2);
    k3_2 = f2(delta1 + 0.5*h*k2_1);

```

```
    k4_1 = f1(delta2 + h*k3_2);
    k4_2 = f2(delta1 + h*k3_1);

    % Update the values of delta1 and delta2 using RK4
    delta1_vals(i+1) = delta1 + (h/6)*(k1_1 + 2*k2_1 + 2*k3_1 + k4_1);
    delta2_vals(i+1) = delta2 + (h/6)*(k1_2 + 2*k2_2 + 2*k3_2 + k4_2);
end

% Interpolation to find t when delta(t) = delta_tc
tc = interp1(delta1_vals, t, delta_tc, 'pchip');
fprintf('The time tc when delta reaches 0.96697 is approximately: %.6f\n', tc
   );

% Plotting resulting waveforms
figure;
plot(t, delta1_vals, 'b', 'LineWidth', 1.5);
hold on;
yline(delta_tc, 'r--', 'Target');
xlabel('Time t');
ylabel('\delta(t)');
title('Solution of the ODE using Runge-Kutta');
ylim([0 3.1]);
grid on;
```

Listing 1: Runge-Kutta method for ODE

References

[1] J. D. Glover, ”Electric Power Distribution,” Encyclopedia of Energy Technology and the Environment, New York, NY: John Wiley & Sons, 1995.

[2] M. Mynuddin, “Stability Study of Power System,” International Journal of Energy and Power Engineering, vol. 4, Feb. 2015, doi: https://doi.org/10.11648/j.ijepe.20150402.15.

[3] T. Bašakarad, N. Holjevac, I. Kuzle, I. ivanković, and N. Zovko, “ROCOF IMPORTANCE IN ELECTRIC POWER SYSTEMS WITH HIGH RENEWABLES SHARE: A SIMULATION CASE FOR CROATIA,” in The 12th Mediterranean Conference on Power Generation, Transmission, Distribution and Energy Conversion (MEDPOWER 2020), pp. 72–77. doi: https://doi.org/10.1049/icp.2021.1239.

[4] Glover/Overbye/Sarma, Power System Analysis and Design, SI Edition. Cengage Learning, 2016.

[5] B. Pepper and D. CamposGaona, "Impedance Estimation for Transient Stability Enhancement of Virtual Synchronous Machines," in 2024 IEEE 15th International Symposium on Power Electronics for Distributed Generation Systems (PEDG), pp. 1–6. doi: https://doi.org/10.1109/PEDG61800.2024.10667411.